CRATER CONCENTRIC RIDGES: KELVIN-HELMHOLTZ INSTABILITIES IN LUNAR EJECTA.
C. Atwood-Stone[1,2], J. McElwaine[3], J. Richardson[4], V.J. Bray[1] and A.S. McEwen[1], [1]Lunar and Planetary, University of Arizona, 1629 E University Blvd., Tucson, AZ 85721, [2]Hinds Community College, Raymond, MS, [3]Department of Earth Sciences, Durham University, UK, [4]Planetary Science Institute, Tucson, AZ..

Introduction & Background: We examine a geologic facies that we have named 'crater concentric ridges' (or CCRs) by comparing geologic data collected by LROC, especially NAC DTMs, with simulated topography produced using Discrete Element Modeling (DEM). This facies is primarily observed around small (1-10 km) craters on the lunar surface [1]. CCRs are short ridges oriented concentrically to their host craters, typically with their tips curving away from the crater, although individual CCRs exhibit considerable morphologic variability [Fig. 1] [2]. In the lunar mare CCRs are distributed fairly evenly around the crater and extend from ~1.2 crater radii out to several crater radii [3]. In the more distal regions these CCRs are often accompanied by downrange troughs or replaced by them altogether. When these features were previously studied [1,4] they were referred to as 'Lunar Concentric Dunes' however we find this name to be misleading as their geomorphic origin does not resemble dune processes and additionally we have observed these ridges on Mercury as well as the Moon [5].

Methodology: We have used numerical modeling to simulate the flow of ejecta over lunar regolith to determine how this facies is formed. In order to do this we have employed the Fortran Discrete Element Method (FDEM) code [6], which was developed for analyzing granular flows. This code simulates the interactions between large numbers of individual particles in order to study the movement and evolution of granular flows.

In this study we are modeling various parameters of ejecta flows as they move over regolith, including velocities, total mass, depth, and particle stream density, in order to examine possible formation mechanisms. These parameters are varied to simulate different distances from the crater in order to capture how CCRs appear at different radial distances.

Our models simulate ejecta flow for small regions at specific distances from the crater to observe how ejecta particles interact both with each other and the particles of the underlying granular regolith as the flow evolves. These regions would feature either a featureless regolith or a small pre-existing crater. Specifically our models are examining flows for crater parameters matching Linné (~2km), Liebig J (~4km) and Piton B (~5km) all of which exhibit the CCR morphology. At each of these craters we consider flow parameters matching different ejecta distances between 1.5 and 4 crater radii. These parameters were determined using the Excavation Flow Properties Model (EFPM) code, which calculates these parameters using crater scaling relationships [7].

In order to determine if these simulations are modeling the processes responsible for the formation of CCRs we compare the topography produced by these models to lunar data. To do this DTMs for several craters which host CCRs were examined and we took topographic profiles of numerous CCRs of different morphologic styles. These profiles were compared with the 2D topographic data produced in our simulations to determine if the simulated flows resemble the topography of real CCRs.

Results: In our simulations we observed the creation of topography from Kelvin-Helmholtz instabilities which form between the ejecta and regolith layers. Kelvin-Helmholtz instabilities are shear instabilities which form between different fluid layers with an initially planar boundary when those layers have different velocities. These instabilities form as small perturbations in the planar boundary are grown due to local pressure differentials, creating a wavelike boundary. After these waveforms grow sufficiently they are rolled over into spirals as a result of the velocity differential [8]. Although this type of instabili-

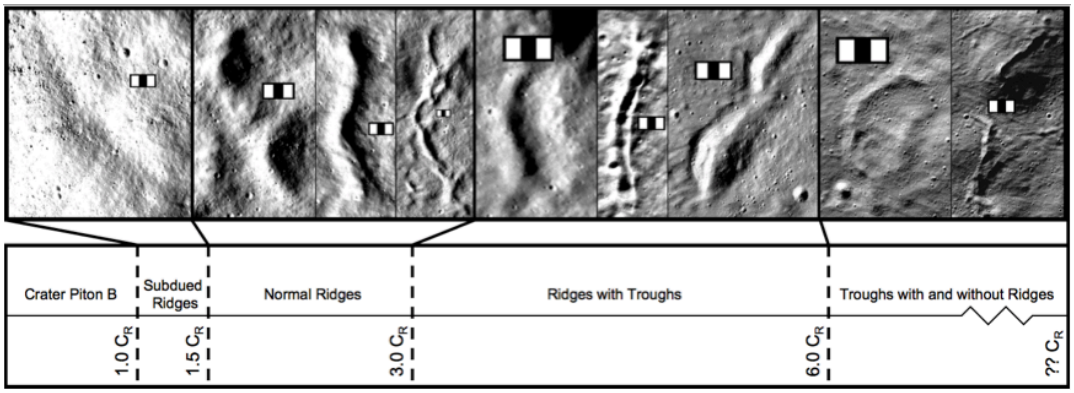

Figure 1: CCR morphology progression. Close up images of CCRs from crater Piton B show how ridge morphology changes with distance from the crater. All images are rotated so that the crater is to the left. The scale bars are all 100 meters long.

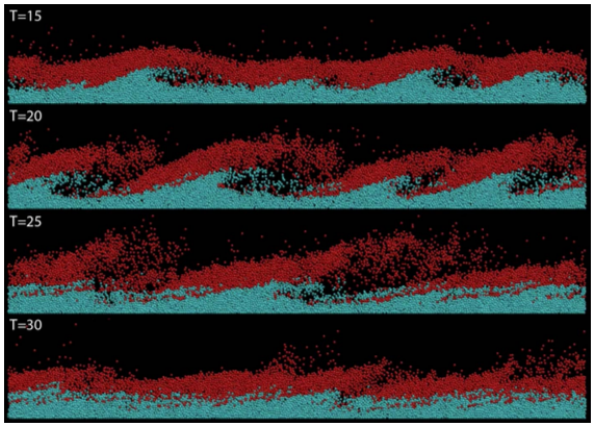

Figure 3: Example timesteps from a simulation where Kelvin-Helmholtz instabilities clearly develop in the ejecta flow. The parameters for this simulation are a rough representation of two crater radii from Linné Crater.

ties is most common between gas or liquid layers, they have been observed to form between granular flows moving at different velocities next to each other moving down inclined planes [9].

In our models these instabilities form between the ejecta and regolith layers, which have significant velocity differential as the regolith is initially at rest [Fig. 2]. These instabilities leave behind remnants of their waveforms as topography after flow in the models has ceased. The formation and character of the Kelvin-Helmholtz instabilities, and the topography they produce, depends significantly on properties of the flow, specifically the initial velocities and the relative depth of ejecta. In slower or shallow flows these instabilities are less pronounced or non-existent. This result matches expectations of real CCRs as they do not form close to the rim, where velocities would be slow, or too far away where the ejecta layer would be very thin.

The formation of Kelvin-Helmholtz instabilities and their resultant topography was also enhanced in those simulations which included a pre-existing crater. This crater, which served as an initial perturbation in the boundary layer, would serve as a catalyst for the formation of the instabilities, and the final topographic features from these simulations were generally larger. This result fits with the discrete nature of real CCRs, as the ejecta flow on the moon would encounter perturbations in the regolith, like pre-existing craters, in different places in all directions which thus causes formation to be enhanced differently in any given direction and distance.

The final topographic features which are formed by our models take on several different morphologic characteristics in the different simulations. The positive topographic features we observe are: individual ridges, sets of small ridges lined up one after another, and large ridges with a small trough in the center. In addition we observe negative topographic features, specifically isolated troughs, and troughs which form directly down range of small ridges. These simulated topographic features all correspond to features of real CCRs shown in our topographic profiles taken from DTMs [Fig. 3]. Further our simulated topography does not include features which are not found in the real topographic profiles and the real topographic profiles do not include additional features which do not appear in the simulations, except in situations that have not been modeled (specifically CCRs forming on underlying slopes).

Conclusions: Our simulations produce topography from ejecta flows that corresponds with topographic observations of real crater concentric ridges on the moon. Additionally, these simulated results also correspond with the observed distribution of CCRs around their host craters. As such we conclude that CCRs are the remnant topography of Kelvin-Helmholtz instabilities which form between flowing ejecta and the granular regolith during crater formation.

References: [1] Morrison & Oberbeck (1975) Proc. Lunar Sci. Conf., 6th:2503-2530. [2] Howard (1974), Proc. of the 5th Lunar Conf. 1:61-69. [3] Melosh (1989), *Impact Cratering: A Geologic Process*. [4] Oberbeck et al. (1975), The Moon, 13:9-26. [5] Atwood-Stone et al. (2016), Icarus 273:196-204. [6] Borzsonyi, Ecke and McElwaine (2009), Phys. Rev. Let. 103:178302. [7] Richardson (2011), JGR Planets, 116:12004. [8] Falkovich (2011), *Fluid mechanics: A Short Course for Physicists*. [9] Goldfarb et al. (2002), 53rd Meeting of Division of Fluvial Dynamics.

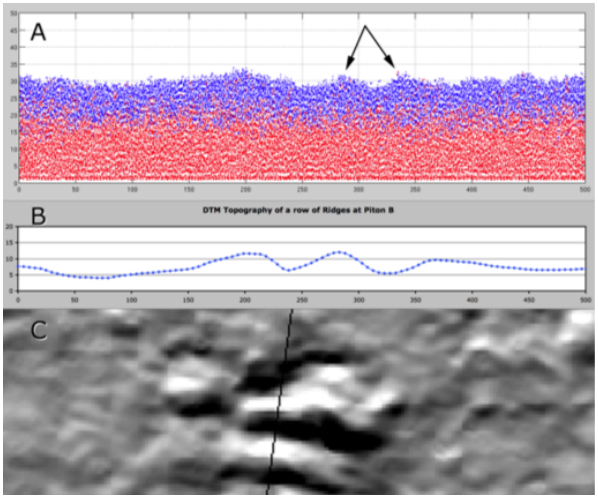

Figure 2: A) Final timestep of a model simulation showing topography of a row of short ridges. B) Topographic profile of a row of CCR ridges at Piton B. C) A NAC image of the CCRs shown in B.